

NMR and X-ray crystallographic studies of axial and equatorial 2-ethoxy-2-oxo-1,4,2-oxazaphosphinane

Irma Linzaga,^{a,b} Jaime Escalante,^b Miguel Muñoz^b and Eusebio Juaristi^{a,*}

^aDepartamento de Química, Centro de Investigación y de Estudios Avanzados del Instituto Politécnico Nacional, Apartado Postal 14-740, 07000 México, DF, Mexico

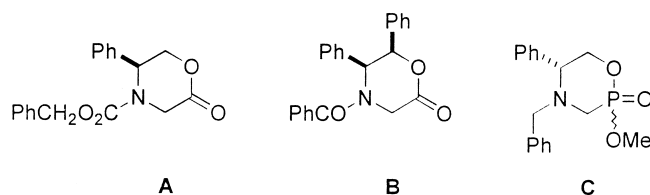
^bCentro de Investigaciones Químicas, Universidad Autónoma del Estado de Morelos, Av. Universidad 1001, Col. Chamilpa, 62210 Cuernavaca, Mor., Mexico

Received 10 July 2002; revised 9 September 2002; accepted 12 September 2002

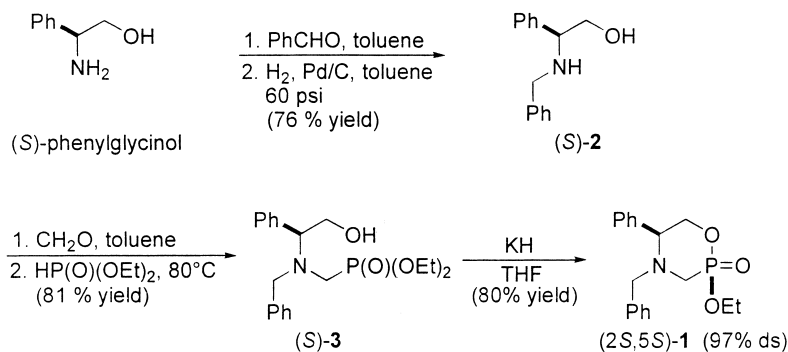
Abstract—Condensation of (*S*)-(*N*-benzyl)-phenylglycinol with formaldehyde in the presence of diethylphosphite afforded hydroxyaminophosphonate (*S*)-**3**, which upon treatment with KH yielded a 97:3 mixture of the interesting, phosphorus-containing 2-ethoxy-2-oxo-1,4,2-oxazaphosphinanes (*2S,5S*)-**1** and (*2R,5S*)-**1**. Suitable crystals of both diastereomers were used in X-ray crystallographic studies that permitted unequivocal configurational assignment, as well as examination of the consequences of $n_{\text{O}} \rightarrow \sigma_{\text{P}-\text{O}}^*$ stereoelectronic interactions on structural properties. © 2002 Elsevier Science Ltd. All rights reserved.

1. Introduction

Some years ago, Dellaria, Williams, and co-workers¹ developed chiral glycine derivatives **A** and **B** as convenient precursors in the enantioselective synthesis of α -substituted α -amino acids. Inspired by this work, and motivated by the large range of biological activities presented by the analogous α -phosphonic acids,^{2,3} Royer et al. recently reported the preparation of oxazaphosphinane derivative **C**.⁴ Nevertheless, compounds **C** were obtained as a 4:1 diastereomeric mixture of epimers at phosphorus, that was not separated into the pure epimers.



In this paper, we describe a highly diastereoselective synthetic procedure for the preparation of enantiopure (*2S,5S*)-4-benzyl-2-ethoxy-2-oxo-5-phenyl-1,4,2-oxazaphosphinane [(*2S,5S*)-**1**] from (*S*)-phenylglycinol (Scheme 1).



Scheme 1.

Keywords: phosphorus heterocycles; diastereoselection; NMR; stereoelectronic effects.

* Corresponding author. Tel.: +52-55-5747-3722; fax: +52-55-5747-7113; e-mail: juaristi@relaq.mx

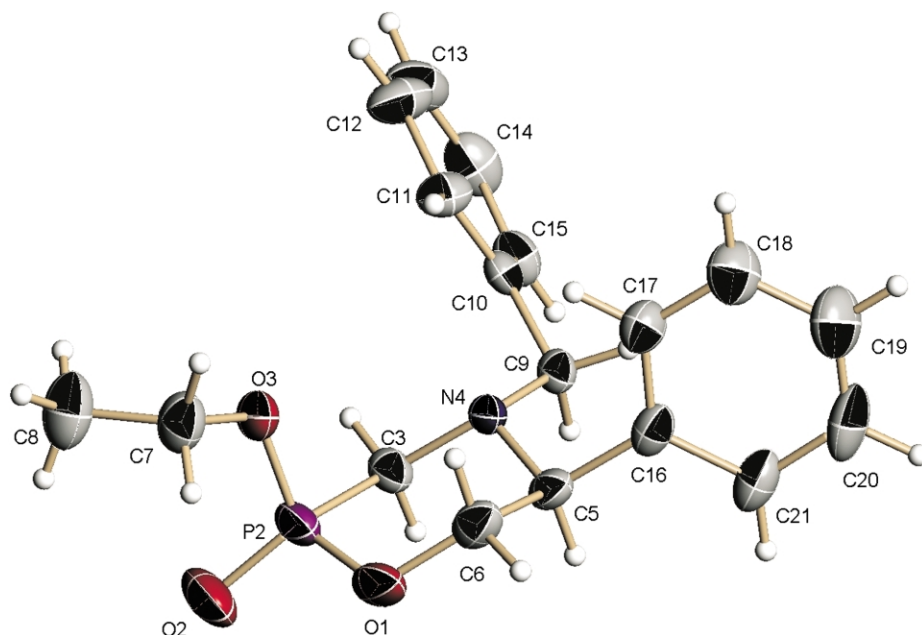


Figure 1. X-Ray crystallographic structure and solid-state conformation of (2*S*,5*S*)-4-benzyl-2-ethoxy-2-oxo-5-phenyl-1,4,2-oxazaphosphinane, (2*S*,5*S*)-**1**.⁹

In addition, isolation of the pure (2*R*,5*S*) epimer permitted comparison of ¹H, ¹³C, and ³¹P NMR data of both isomers. Finally, suitable crystals of both (2*S*,5*S*)-**1** and (2*R*,5*S*)-**1** were subjected to X-ray crystallographic analysis. This study not only secured the assignment of configuration based on infrared and NMR data, but afforded relevant information on the stereoelectronic interactions that may account for the increased stability of (2*S*,5*S*)-**1** (axial *P*-ethoxy group).

2. Results and discussion

2.1. Preparation of oxazaphosphinane 2-oxides (2*S*,5*S*)-**1** and (2*R*,5*S*)-**1**

N-Benzylation of (*S*)-phenylglycinol was achieved by condensation with benzaldehyde followed by palladium-catalyzed hydrogenation.⁵ *N*-Benzyl-(*S*)-phenylglycinol, (*S*)-**2**, was then condensed with formaldehyde (toluene

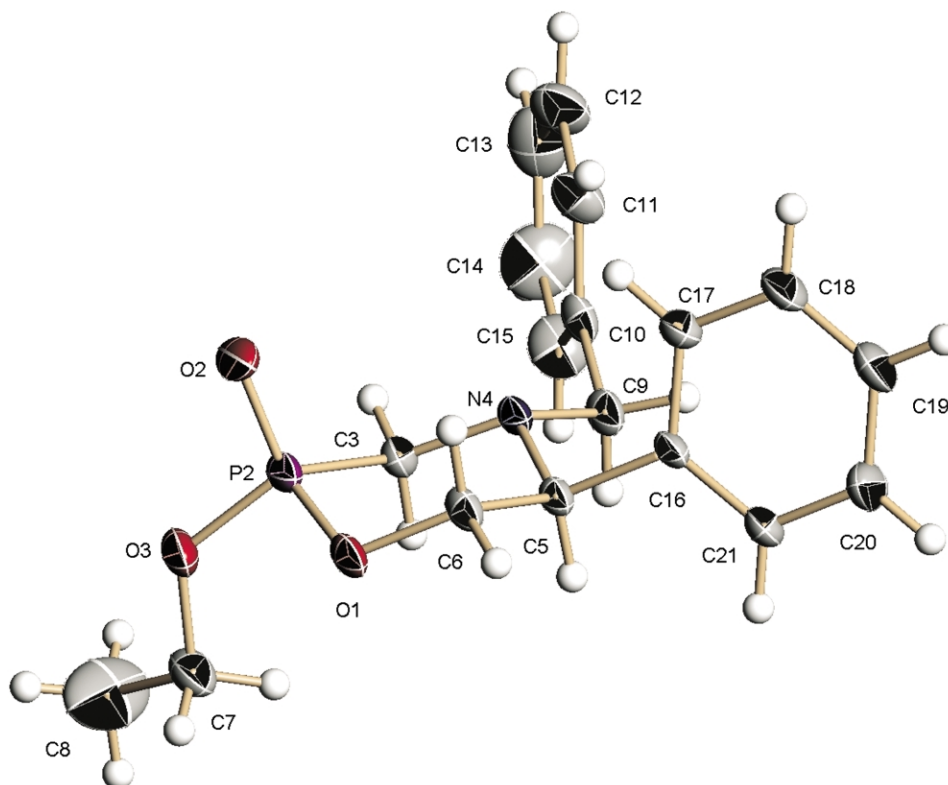


Figure 2. X-Ray crystallographic structure and solid-state conformation of (2*R*,5*S*)-4-benzyl-2-ethoxy-2-oxo-5-phenyl-1,4,2-oxazaphosphinane, (2*R*,5*S*)-**1**.⁹

solvent) and the resulting imminium salt was immediately treated with diethyl phosphite to afford Mannich product (*S*)-**3** in 81% isolated yield.⁶

Treatment of carbinol (*S*)-**3** with KH in THF solution afforded in good yield and high diastereoselectivity the cyclization products 1,4,2-oxazaphosphinanes (*2S,5S*)-**1** and (*2R,5S*)-**1**, in a 97:3 ratio (Scheme 1). Separation of these diastereomeric phosphorus-containing heterocycles was feasible by means of flash column chromatography, and unequivocal assignment of configuration was achieved by X-ray diffraction structural determination.

That the 97:3 ratio of cyclized derivatives (*2S,5S*)-**1** and (*2R,5S*)-**1** is the result of kinetic rather than thermodynamic control is inferred by the fact that treatment of either diastereomer with KH in THF for two hours and at -75°C (i.e. the same conditions employed for the cyclization reaction) afforded no epimerized product.

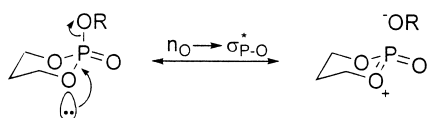
The crystallographic data of (*2S,5S*)-**1** and (*2R,5S*)-**1** were also of significant interest with regard the possible manifestation of stereoelectronic interactions in O–P=O and O–P–OEt segments.^{7,8} Furthermore, the availability of both diastereomeric oxazaphosphinanes in pure form permitted evaluation of the spectroscopic criteria that are usually examined for the configurational assignment at phosphorus.⁸

2.2. X-Ray crystallographic structural analysis of (*2S,5S*)-**1** and (*2R,5S*)-**1**

Figs. 1 and 2 present the solid-state conformations that were determined by X-ray diffraction analysis of suitable crystals of (*2S,5S*)-**1** and (*2R,5S*)-**1**, respectively.

Salient features in the crystallographic structures (Figs. 1 and 2) are the chair conformation of the six-membered heterocyclic rings and the anchoring effect of the phenyl substituent at C(5),^{10,11} that is reflected in an axial or equatorial orientation of the P=O phosphoryl group in (*2R,5S*)-**1** and (*2S,5S*)-**1**, respectively. Of course, since the absolute configuration at C(5) is (*S*), then determination of the relative configuration at phosphorus establishes the absolute configuration of this center of chirality as well.

X-Ray crystallography has proved to be a powerful tool to reveal the effect of substituent orientation on phosphorus in 1,3,2-dioxaphosphorinanes on critical bond lengths and angles about phosphorus.¹² In particular, hyperconjugative stereoelectronic $n_{\text{O}} \rightarrow \sigma_{\text{P-OEt}}^*$ interaction is expected to be reflected in longer P–OEt bond length when the ethoxy group is axial, relative to equatorial P–OEt. The double bond–no bond canonical structure that results from $n_{\text{O}} \rightarrow \sigma_{\text{P-OEt}}^*$ hyperconjugation (Scheme 2) is also consistent with the shorter $\text{O}_{\text{ring}}\text{-P}$ bond that is usually observed in the



Scheme 2.

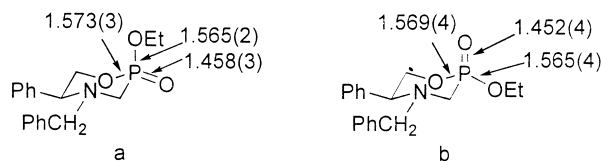
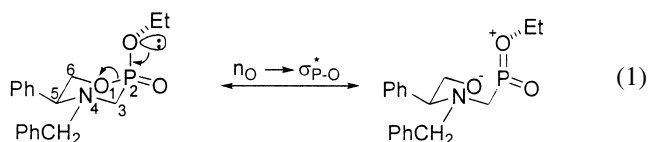


Figure 3. P–O bond lengths Å in diastereomeric (a) (*2S,5S*)-**1** and (b) (*2R,5S*)-**1**.

isomer presenting the axial P–OR substituent (Scheme 2).^{8, 12–14}

Unexpectedly, all three relevant P–O bond lengths present in diastereomeric (*2S,5S*)-**1** and (*2R,5S*)-**1** are identical, within the experimental margin of error (Fig. 3).

We initially considered the possibility that a dominant *exo* anomeric interaction¹³ in (*2S,5S*)-**1** relative to (*2R,5S*)-**1** could be responsible for elongation of the endocyclic P–O bond in the former, as consequence of $n_{\text{OEt}} \rightarrow \sigma_{\text{P-O(1)}}^*$ hyperconjugation (Eq. (1)).



Nevertheless, examination of the X-ray crystallographic structures (Figs. 1 and 2) helps discard this hypothesis, since it is the O–Et bond in (*2S,5S*)-**1** rather than the lone pair at oxygen that is more closely antiperiplanar to P–O(1): $\tau = 140.8^{\circ}$ (Fig. 4(a)). By contrast, one of the lone electron pairs at oxygen in the equatorial O–Et isomer (*2R,5S*)-**1** can be located at $\tau = 170.7^{\circ}$, i.e. an almost ideal orientation for the anticipated $n_{\text{OEt}} \rightarrow \sigma_{\text{P-O(1)}}^*$ stereoelectronic interaction (Fig. 4(b)).

It can be appreciated in Fig. 4, that one of the oxygen lone pairs in (*2S,2S*)-**1** (axial P–OEt) should be nearly eclipsed with the long P–O(1) endocyclic bond (estimated dihedral angle between the exocyclic sp^3 -hybridized lone pair and the endocyclic P–O(1) bond is equal to 20.8°). It could be argued that *syn*-periplanar $n_{\text{OEt}} \rightarrow \sigma_{\text{P-O(1)}}^*$ hyperconjugation in the nearly *syn* arrangement leads to the observed lengthening in the acceptor orbital.¹³ (Eq. (2)), counterbalancing the normal

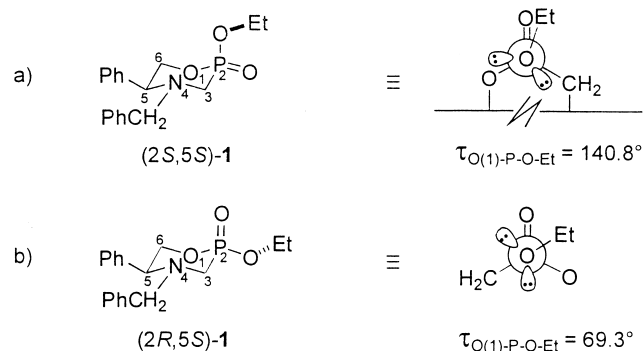
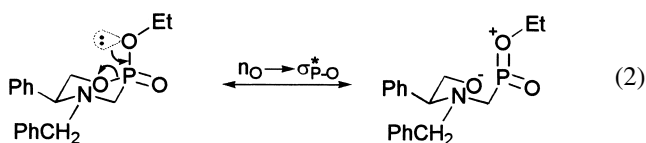


Figure 4. Dihedral angles for the O(1)–P–O–Et segments in epimeric oxazaphosphinanes (*2S,2S*)-**1** and (*2R,2S*)-**1**, as determined from the X-ray crystallographic structures (Figs. 1 and 2).

antiperiplanar $n_{O(1)} \rightarrow \sigma_{P-OEt}^*$ hyperconjugative interaction.



2.3. Infrared and multinuclear NMR analysis of (2*S*,5*S*)-1 and (2*R*,5*S*)-1

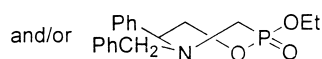
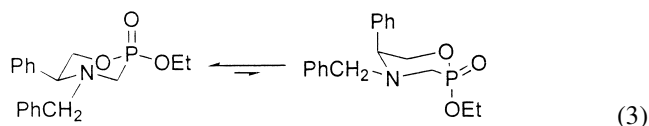
The most useful criteria for assigning configuration at phosphorus in individual diastereomers of 1,3,2-dioxaphosphorinanes include infrared frequencies for the P=O stretch and relative ^{31}P chemical shifts.⁸ For the P=O stretch one finds $\nu(\text{P}=\text{O}_{\text{eq}}) > \nu(\text{P}=\text{O}_{\text{ax}})$,¹⁵ and this trend is also evident in diastereomeric (2*S*,5*S*)-1 with $\nu=1261\text{ cm}^{-1}$ (equatorial phosphoryl), and (2*R*,5*S*)-1 with $\nu=1225$ and 1256 cm^{-1} (axial phosphoryl).¹⁶

With regard ^{31}P NMR chemical shifts, an extensive list of data for 1,3,2-diheterophosphorinanes has been compiled in Ref. 17, showing that $\delta^{31}\text{P}(\text{P}=\text{O}_{\text{ax}}) > \delta^{31}\text{P}(\text{P}=\text{O}_{\text{eq}})$.¹⁷ This trend is also found in epimeric 2-oxo-1,4,2-oxazaphosphinane (2*S*,5*S*)-1 and (2*R*,5*S*)-1, where $\delta^{31}\text{P}(\text{P}=\text{O}_{\text{ax}})=20.3\text{ ppm}$ and $\delta^{31}\text{P}(\text{P}=\text{O}_{\text{eq}})=19.4\text{ ppm}$.

Finally, a remarkable similarity in ^1H and ^{13}C NMR data for (2*S*,5*S*)-1 and (2*R*,5*S*)-1 is evident. (Figs. 5 and 6). As noted

by Royer and co-workers,⁴ perhaps the most distinctive feature for the proton NMR spectra is the smaller $^3J_{\text{P/H}(6_{\text{ax}})}$ (2.5 vs. 7.2 Hz) and larger $^3J_{\text{P/H}(6_{\text{eq}})}$ (21.9 vs. 17.4 Hz) coupling constants in the major (2*S*,5*S*) isomer.

A salient observation from Fig. 5 is that, whereas $^3J_{\text{anti}}$ for H(6) in (2*S*,5*S*)-1, i.e. axial P–OEt isomer is a normal 11.1 Hz, in the equatorial (2*R*,5*S*)-1 compound is only 8.4 Hz. This suggests a possible conformational equilibrium in the latter, with appreciable amounts of either an inverted chair (axial P–OEt and axial phenyl group) or a twist-boat conformation (Eq. (3)).



Comparison of the ^{13}C NMR data for (2*S*,5*S*)-1 and (2*R*,5*S*)-1 (Fig. 6) indicates an absence of the γ -gauche upfield shift¹⁸ at C(3) in the latter isomer. This finding, together with evidence of a deformed chair in the X-ray crystallographic structure of (2*S*,5*S*)-1 (Fig. 2; for example, the ring torsion angle N(4)–C(3)–P(2)–O(1)= $52.9(4)^\circ$ in (2*R*,5*S*)-1 is significantly larger than $\tau_{\text{N}(4)-\text{C}(3)-\text{P}(2)-\text{O}(1)}=46.8(2)^\circ$ for (2*S*,5*S*)-1). Thus it is apparent that the absence of the $n_{O(1)} \rightarrow \sigma_{\text{P-OEt}}^*$ anomeric effect in chair-shaped (2*R*,5*S*)-1 causes a destabilization,

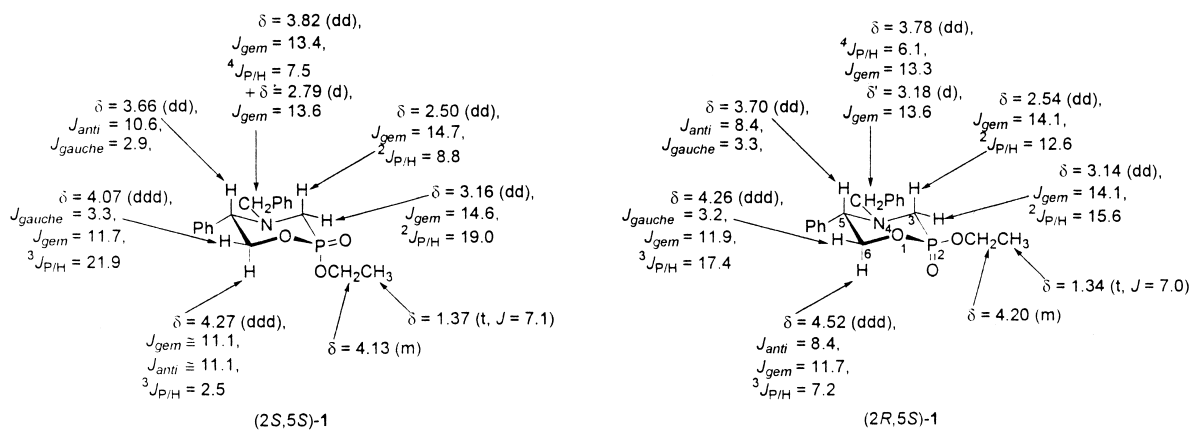


Figure 5. Relevant ^1H NMR chemical shifts (ppm) and coupling constants (Hz) in (2*S*,5*S*)-1 and (2*R*,5*S*)-1, at 400 MHz.

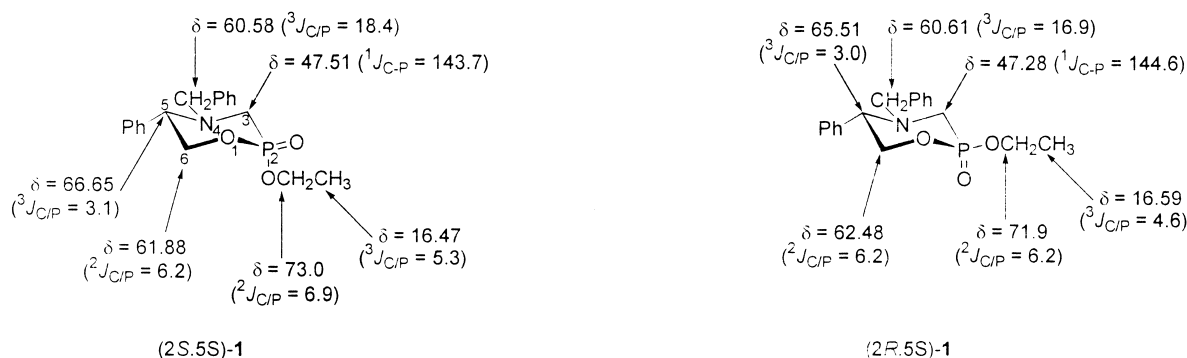


Figure 6. Relevant ^{13}C NMR chemical shifts (ppm) and coupling constants (Hz) in (2*S*,5*S*)-1 and (2*R*,5*S*)-1, at 100 MHz.

which pushes the ring in the direction of a twist-boat conformation.

3. Concluding remarks

As evidenced by Royer's observations,⁴ the method of synthesis presented in this report should be applicable when other aldehydes are employed in place of formaldehyde, providing ready access to alkylated analogs of phosphonic acids. Furthermore, given the availability of both isomers of **1**, it should be possible to find conditions to deprotonate and alkylate either isomer to gain access to the analogs noted above. We are currently pursuing these objectives.

4. Experimental

4.1. General

Flasks, stirring bars, and hypodermic needles used for the generation and reactions of organolithiums were dried for about 12 h at 120°C. Anhydrous THF was obtained by distillation from benzophenone ketyl. The butyllithium employed was titrated according to the method of Juaristi et al. (4-biphenylmethanol indicator).¹⁹ TLC, F₂₅₄ silica gel plates; detection by UV light or iodine vapor. Flash column chromatography: silica gel (230–400 mesh). All melting points are uncorrected. ¹H NMR spectra: JEOL FX-90Q (90 MHz), JEOL GSX-270 (270 MHz), and JEOL Eclipse-400 (400 MHz) spectrometers. ¹³C NMR spectra: JEOL FX-90Q (22.5 MHz), JEOL GSX-270 (67.8 MHz), and JEOL Eclipse-400 (100 MHz) spectrometers. Optical rotations were measured in a Perkin–Elmer Model 241 polarimeter, using the sodium D-line (589 nm). Elemental analyses were performed by Galbraith Laboratories, Inc., TN. The purity of new compounds, for which elemental analyses are not provided, was judged to be >97%, as evidenced by ¹H and ¹³C NMR spectra.

4.1.1. (S)-2-(Benzylamino)-2-phenylethanol, (S)-2. (S)-Phenylglycinol (1.9 g, 13.8 mmol) was placed in a 50-mL three-neck round-bottom flask fitted with a magnetic stirbar, a Dean–Stark trap, and a reflux condenser. Toluene (20 mL) and 1.46 g (13.7 mmol) of benzaldehyde were added to the flask, and the reaction mixture was heated to reflux for 30 min and then allowed to cool to room temperature. The resulting imine mixture was immediately treated with 0.31 g of 10% palladium on charcoal and shaken in a Parr apparatus during 2.5 h under 60 psi of hydrogen pressure. After removal of the catalyst by filtration over celite and evaporation of the solvent, the crude product was recrystallized from methylene chloride–hexane (1:9) to give 2.4 g (76% yield) of the desired product as a white solid: mp 86–87°C (lit.⁴ mp 88°C). $[\alpha]_{\text{D}}^{28} = +83.2$ ($c = 1.6$, EtOH) lit.⁴ $[\alpha]_{\text{D}} = -82.5$ ($c = 1$, CHCl₃) for the (R) enantiomer.

4.1.2. {[Benzyl-(2-hydroxy-1S-phenyl-ethyl)-amino]-methyl}-phosphonic acid diethyl ester, (S)-3. N-Benzylated (S)-phenylglycinol, (S)-2, (2.29 g, 10.0 mmol) was placed in a 50-mL round-bottom flask and dissolved in 25 mL of toluene before the addition of 0.82 mL of an aqueous 37% solution of formaldehyde (0.03 g, 10 mmol).

The flask was fitted with a Dean–Stark trap and the reaction mixture was heated to reflux for 30 min with removal of water. The flask was allowed to cool to ambient temperature before the addition of 1.39 g (10 mmol) of diethyl phosphite, and the reaction mixture was heated to 80°C for 4 h. The solvent was removed in a rotary evaporator and the residue was purified by flash chromatography (ethyl acetate–hexane, 8:2→6:4) to give 2.75 g (81% yield) of aminophosphonate (S)-**3** as a colorless liquid: $[\alpha]_{\text{D}}^{28} = +66.6$ ($c = 1.42$, CHCl₃). IR (cm⁻¹) ν 3397, 1663, 1217, 1027. ¹H NMR (CDCl₃, 400 MHz) δ 1.29 and 1.34 (2xt, 6H, $J_{\text{vic}} = 7.0$ Hz), 2.68 (dd, 1H, $J_{\text{gem}} = 15.7$ Hz, $^2J_{\text{H/P}} = 3.3$ Hz), 3.26 (dd, 1H, $J_{\text{gem}} = 16.1$ Hz, $^2J_{\text{H/P}} = 17.2$ Hz), 3.46 (d, 1H, $J_{\text{gem}} = 13.8$ Hz), 3.65 (dd, 1H, $J_{\text{gem}} = 11.0$ Hz, $^4J_{\text{H/P}} = 18.7$ Hz), 4.0 (s, 1H), 4.06 (masked, 1H), ca. 4.1 (masked, 1H), 4.14 (masked, 4H), 7.18–7.44 (m, 10H). ¹³C NMR (CDCl₃, 100 MHz) δ 16.5 (d, $^3J_{\text{C/P}} = 5.4$ Hz), 45.0 (d, $^1J_{\text{C/P}} = 167.6$ Hz), 56.7 (d, $^4J_{\text{C/P}} = 5.4$ Hz), 61.75, 62.2 (d, $J = 6.9$ Hz), 64.3, 127.3, 127.9, 128.5, 128.5, 128.8, 128.9, 135.9, 138.5. ³¹P NMR (CDCl₃, 161.8 MHz) δ 27.9. HRMS calcd for C₂₀H₂₈NO₄P (M⁺+1): 378.1834. Found: 378.1831.

4.1.3. (2R,5S)- and (2S,5S)-4-Benzyl-2-ethoxy-2-oxo-5-phenyl-1,4,2-oxazaphos-phinane, (2R,5S)-1 and (2S,5S)-1. In a 50-mL round-bottom flask fitted with rubber septa and under nitrogen atmosphere, potassium hydride (65.7 mg, 1.64 mmol) was suspended in 15 mL of dry THF. The flask was cooled to –75°C in a dry ice-acetone bath before the addition of 619 mg (1.64 mmol) of aminophosphonate (S)-**3** in 9 mL of dry THF. The reaction mixture was allowed to react at –75°C for 2 h before quenching with 20 mL of brine solution. The organic product was extracted with three 15-mL portions of ethyl acetate; dried over anh. sodium sulfate, and evaporated in a rotary evaporator. ³¹P NMR analysis of the crude product showed a 97:3 mixture of the expected diastereomeric products (431 mg, 79% yield), which were separated by flash chromatography (hexane–ethyl acetate, 75:25). Recrystallization from hexane–CH₂Cl₂ (4:1) afforded crystals suitable for X-ray diffraction analysis.

(2R,5S)-**1**: mp 138–140°C; $[\alpha]_{\text{D}}^{28} = -33.9$ ($c = 1.09$, CHCl₃). IR (cm⁻¹) ν 1256, 1047. ¹H NMR (CDCl₃, 400 MHz) δ 1.34 (t, 3H, $J_{\text{vic}} = 7.0$ Hz), 2.54 (dd, 1H, $J_{\text{gem}} = 14.1$ Hz, $^2J_{\text{H/P}} = 12.6$ Hz), 3.14 (dd, 1H, $J_{\text{gem}} = 14.1$ Hz, $^2J_{\text{H/P}} = 15.6$ Hz), 3.18 (d, 1H, $J_{\text{gem}} = 13.6$ Hz), 3.70 (dd, 1H, $J_{\text{anti}} = 8.4$ Hz, $J_{\text{gauche}} = 3.3$ Hz), 3.78 (dd, 1H, $J_{\text{gem}} = 13.3$ Hz, $^4J_{\text{H/P}} = 6.1$ Hz), 4.20 (m, 2H), 4.26 (ddd, 1H, $J_{\text{gem}} = 11.9$ Hz, $J_{\text{gauche}} = 3.2$ Hz, $^3J_{\text{H/P}} = 17.4$ Hz), 4.52 (ddd, 1H, $J_{\text{gem}} = 11.7$ Hz, $J_{\text{anti}} = 8.4$ Hz, $^3J_{\text{H/P}} = 7.2$ Hz), 7.22–7.50 (m, 10H). ¹³C NMR (CDCl₃, 100 MHz) δ 16.6 (d, $^3J_{\text{C/P}} = 4.6$ Hz), 47.3 (d, $^1J_{\text{C/P}} = 144.6$ Hz), 60.6 (d, $^3J_{\text{C/P}} = 16.9$ Hz), 62.48 (d, $^2J_{\text{C/P}} = 6.2$ Hz), 65.5 (d, $^3J_{\text{C/P}} = 3.0$ Hz), 71.9 (d, $^2J_{\text{C/P}} = 6.2$ Hz), 127.4, 128.5, 128.7, 129.0, 136.7, 137.0; ³¹P NMR (CDCl₃, 161.8 MHz) δ 20.3. X-Ray crystallographic structure in Fig. 2.⁹ Anal. calcd for C₁₈H₂₂NO₃P: C, 65.24; H, 6.69; N, 4.22. Found: C, 65.58; H, 5.92; N, 3.95.

(2S,5S)-**1**: mp 92–94°C. $[\alpha]_{\text{D}}^{28} = +31.0$ ($c = 1.03$, CHCl₃). IR (cm⁻¹) ν 1261, 1039. ¹H NMR (CDCl₃, 400 MHz) δ 1.37 (t, 3H, $J_{\text{vic}} = 7.1$ Hz), 2.50 (dd, 1H, $J_{\text{gem}} = 14.7$ Hz, $^2J_{\text{H/P}} = 8.8$ Hz), 2.93 (d, 1H, $J_{\text{gem}} = 13.6$ Hz), 3.16 (dd, 1H,

$J_{gem}=14.6$ Hz, ${}^2J_{HP}=19.0$ Hz), 3.66 (dd, 1H, $J_{anti}=10.6$ Hz, $J_{gauche}=2.9$ Hz), 3.82 (dd, 1H, $J_{gem}=13.4$ Hz, ${}^4J_{HP}=7.5$ Hz), 4.07 (ddd, 1H, $J_{gem}=11.7$ Hz, $J_{gauche}=3.3$ Hz, ${}^3J_{HP}=21.9$ Hz), 4.13 (m, 2H), 4.27 (ddd, $J_{gem}\cong 11.1$ Hz, $J_{anti}\cong 11.1$ Hz, ${}^3J_{HP}=2.5$ Hz), 7.20–7.46 (m, 10H). ${}^{13}\text{C}$ NMR (CDCl_3 , 100 MHz) δ 16.5 (d, ${}^3J_{CP}=5.3$ Hz), 47.5 (d, ${}^1J_{CP}=143.7$ Hz), 60.6 (d, ${}^3J_{CP}=18.4$ Hz), 61.9 (d, ${}^2J_{CP}=6.2$ Hz), 66.7 (d, ${}^3J_{CP}=3.1$ Hz), 73.0 (d, ${}^2J_{CP}=6.9$ Hz), 127.5, 128.3, 128.5, 128.7, 128.7, 129.1, 136.9, 137.0. ${}^{31}\text{P}$ NMR (CDCl_3 , 161.8 MHz) δ 19.4. X-Ray crystallographic structure in Fig. 1.⁹ Anal. calcd for $\text{C}_{18}\text{H}_{22}\text{NO}_3\text{P}$: C, 65.24; H, 6.69; N, 4.22. Found: C, 65.04; H, 6.71; N, 4.17.

Acknowledgements

We are indebted to Conacyt, México, for financial support via grant 33023-E, and to M. L. Kaiser-Carril for technical assistance. We are also grateful to the referees for many important suggestions.

References

- (a) Dellaria, J. F.; Santarsiero, B. D. *J. Org. Chem.* **1989**, *54*, 3916. (b) Williams, R. M.; Sinclair, P. J.; Zhai, D.; Chen, D. *J. Am. Chem. Soc.* **1988**, *110*, 1547.
- For some articles concerning the biological activity of α -aminophosphonic acid derivatives, see: (a) Huang, J.; Chen, R. *Heteroat. Chem.* **2000**, *11*, 480; and references therein. (b) Kafarski, P.; Lejczak, B. *Phosphorus Sulfur Silicon Relat. Elem.* **1991**, *63*, 193; and references therein.
- For examples of enantioselective synthesis of α -alkylated α -aminophosphonic acids, see: (a) Yuan, C.; Li, S.; Wang, G. *Heteroat. Chem.* **2000**, *11*, 528. (b) Sawamura, M.; Hamashima, H.; Ito, Y. *Bull. Chem. Soc. Jpn* **2000**, *73*, 2559. (c) Gröger, H.; Saida, Y.; Sasai, H.; Yamaguchi, K.; Martens, J.; Shibasaki, M. *J. Am. Chem. Soc.* **1998**, *120*, 3089. (d) Kukhar, V. P.; Soloshonok, V. A.; Solodenko, V. A. *Phosphorus Sulfur Silicon Relat. Elem.* **1994**, *92*, 239. (e) Dhawan, B.; Redmore, D. *Phosphorus Sulfur* **1987**, *32*, 119. (f) Schöllkopf, U.; Schütze, R. *Liebigs Ann. Chem.* **1987**, 45.
- Maury, C.; Gharbaoui, T.; Royer, J.; Husson, H. P. *J. Org. Chem.* **1996**, *61*, 3687.
- Cf. Eleveld, M. B.; Hogeveen, H.; Schudde, E. P. *J. Org. Chem.* **1986**, *51*, 3635.
- For a general procedure, see: Fields, E. K. *J. Am. Chem. Soc.* **1952**, *74*, 1528.
- Gorenstein, D. G. *Chem. Rev.* **1987**, 1047; and references cited therein.
- Bentrude, W. G. Steric and Stereoelectronic Effects in 1,3,2-Dioxaphosphorinanes. In *Conformational Behavior of Six-Membered Rings. Analysis, Dynamics, and Stereoelectronic Effects*. Juaristi, E., Ed.; VCH: New York, 1995; pp 245–293 Chapter 7.
- Atomic coordinates for all the structures reported in this paper have been deposited with the Cambridge Crystallographic Data Centre. The coordinates can be obtained, on request, from the Director, Cambridge Crystallographic Centre, 12 Union Road, Cambridge CB2 1EZ, UK.
- The conformational free energy difference of a phenyl group in cyclohexane (A -value¹¹) amounts to ca. 2.9 kcal/mol. See: Eliel, E. L.; Manoharan, M. *J. Org. Chem.* **1981**, *46*, 1959. See, also: Bushweller, C. H. Stereodynamics of Cyclohexane and Substituted Cyclohexanes. Substituent A Values. In *Conformational Behavior of Six-Membered Rings. Analysis, Dynamics, and Stereoelectronic Effects*. Juaristi, E., Ed.; VCH: New York, 1995; pp 25–58 Chapter 2.
- (a) Juaristi, E. *Introduction to Stereochemistry and Conformational Analysis*. Wiley: New York, 1991. (b) Eliel, E. L.; Wilen, S. H.; Mander, L. N. *Stereochemistry of Organic Compounds*. Wiley: New York, 1994.
- Van Nuffel, P.; Van Alsenoy, C.; Lenstra, A. T. H.; Geise, H. J. *J. Mol. Struct.* **1984**, *125*, 1.
- (a) Juaristi, E.; Cuevas, G. *Tetrahedron* **1992**, *48*, 5019. (b) In *The Anomeric Effect and Associated Stereoelectronic Effects*. Thatcher, G. R. J., Ed.; American Chemical Society: Washington, 1993. (c) Graczyk, P. P.; Mikolajczyk, M. *Top. Stereochem.* **1994**, *21*, 159. (d) Juaristi, E.; Cuevas, G. *The Anomeric Effect*. CRC: Boca Raton, FL, 1995.
- Setzer, W. N.; Bentrude, W. G. *J. Org. Chem.* **1991**, *56*, 7212.
- Maryanoff, B. E.; Hutchins, R. O.; Maryanoff, C. S. *Top. Stereochem.* **1979**, *11*, 187.
- In a closely related system, 4,5-dimethyl-2-ethoxy-2-oxo-1,2-oxaphosphorinane, Bergesen and Vikane report $\nu(\text{P}=\text{O}_{\text{eq}})=1256$ cm^{-1} and $\nu(\text{P}=\text{O}_{\text{ax}})=1237$ and 1250 cm^{-1} . Bergesen, K.; Vikane, T. *Acta Chem. Scand.* **1972**, *26*, 1794.
- Gallagher, M. J. Conformation and Stereochemistry of Cyclic Compounds. In *Phosphorus-31 NMR Spectroscopy in Stereochemical Analysis*. Verkade, J. G., Quin, L. D., Eds.; VCH: Deerfield Beach, FL, 1987; pp 297–330 Chapter 9.
- (a) Grant, D. M.; Cheney, B. V. *J. Am. Chem. Soc.* **1967**, *89*, 5315. (b) Wilson, N. K.; Stothers, J. B. *Top. Stereochem.* **1973**, *8*, 1.
- Juaristi, E.; Martínez-Richa, A.; García-Rivera, A.; Cruz-Sánchez, J. S. *J. Org. Chem.* **1983**, *48*, 2603.